ACS Catalysis

Research Article

pubs.acs.org/acscatalysis

Selective Photocatalytic Oxidation of Aniline to Nitrosobenzene by Pt Nanoparticles Supported on TiO_2 under Visible Light Irradiation

Yasuhiro Shiraishi,*[,†] Hirokatsu Sakamoto,[†] Keisuke Fujiwara,[†] Satoshi Ichikawa,[‡] and Takayuki Hirai[†]

[†]Research Center for Solar Energy Chemistry and Division of Chemical Engineering, Graduate School of Engineering Science, Osaka University, Toyonaka 560-8531, Japan

[‡]Institute for NanoScience Design, Osaka University, Toyonaka 560-8531, Japan

Supporting Information

ABSTRACT: Visible light irradiation (λ > 450 nm) of Pt nanoparticles supported on Degussa P25 TiO_2 (Pt/P25 catalyst) promotes efficient and selective aerobic oxidation of aniline to nitrosobenzene. This is facilicated via the interband excitation of Pt atoms by visible light followed by the transfer of activated electrons to the TiO_2 conduction band. The positive charges formed on the Pt surface oxidize substrates, and the conduction band electrons reduce O_2, promoting photocatalytic cycles. The high activity of Pt/P25 is due to the high electron density of Pt particles. They behave as Lewis base sites for reductive deprotonation of aniline, thus promoting efficient aniline oxidation. The Pt/P25 catalyst, when photoirradiated at a low temperature (~283 K), suppresses subsequent condensation of aniline and the formed nitrosobenzene, successfully producing nitrosobenzene with a very high selectivity (90%).

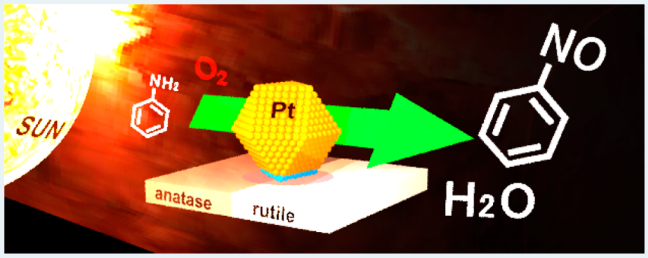

KEYWORDS: *photocatalysis, visible light, platinum, nanoparticles, titanium dioxide*

INTRODUCTION

Nitrosobenzene is a versatile intermediate for organic synthesis in several reactions such as aldol,[1] ene,[2] and Diels–Alder[3] reactions. Traditionally, this compound is synthesized by oxidation of aniline with an excess of unstable peracids such as peracetic acid and perbenzoic acid.[4−6] Catalytic oxidation with a phosphotungstate or phosphomolybdate catalyst has also been proposed;[7−9] however, these methods require expensive hydrogen peroxide as an oxidant. Aerobic oxidation of aniline with molecular oxygen (O_2) as an oxidant (eq 1) is therefore an ideal process from the viewpoint of green chemistry. Some catalytic systems have been proposed;[10−12] however, they require high temperatures (>373 K). The high-temperature reactions inevitably promote subsequent condensation of aniline with the formed nitrosobenzene[13,14] and produce azobenzene as a main product (eq 2). A new catalytic system that promotes aerobic oxidation of aniline at low temperatures is therefore necessary for selective production of nitrosobenzene.

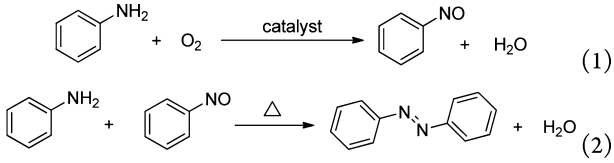

Photocatalytic oxidation on semiconductor materials with O_2 is one of the possible methods that can serve this purpose because the reaction proceeds under photoirradiation even at room temperature.[15−18] There have been three reports of photocatalytic oxidation of aniline with O_2.[19−21] These systems employed a titanium dioxide (TiO_2), zinc oxide (ZnO), or zirconium dioxide (ZrO_2) semiconductor catalyst under UV irradiation. All of these systems, however, produce azobenzene as a major product, where nitrosobenzene is scarcely detected during the reactions.

Earlier, we reported that gold (Au)[22,23] or platinum (Pt)[24,25] nanoparticles supported on TiO_2 successfully promote aerobic oxidation of alcohols to aldehydes under visible light irradiation (λ > 450 nm). Scheme 1 summarizes the mechanism for photoreaction occurring in the Pt/TiO_2 system. Visible light absorption of Pt particles promotes an interband transition of 5d band electrons (e^-). The e^- overcome the Schottky barrier (ϕ_B) created at the Pt–TiO_2 heterojunction[26] and are transferred to the TiO_2 conduction band.[27] The positive charges formed on the surface of Pt particles oxidize the substrate, while the e^- on TiO_2 are consumed by the reduction of O_2. This catalytic cycle successfully promotes aerobic oxidation of alcohols even at room temperature.

In the work presented here, Pt particles supported on TiO_2 (Pt/TiO_2 catalysts) were used for photocatalytic oxidation of aniline with O_2 under visible light irradiation (>450 nm). We found that Pt particles supported on Degussa P25 TiO_2, a

Received: April 4, 2014
Revised: May 16, 2014
Published: June 16, 2014

   dx.doi.org/10.1021/cs500447n | ACS Catal. 2014, 4, 2418−2425

Scheme 1. Proposed Mechanism for the Transfer of an Electron from Photoactivated Pt Particles to TiO_2[a]

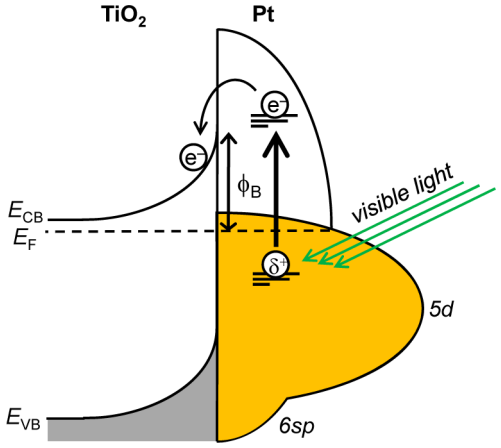

[a] E_{CB}, E_{VB}, E_F, and ϕ_B denote the conduction band potential, valence band potential, Fermi level, and the height of the Schottky barrier, respectively.

mixture of anatase and rutile particles,[28−30] promote efficient nitrosobenzene production. X-ray photoelectron spectroscopy (XPS) and diffuse-reflectance infrared Fourier transform (DRIFT) analysis revealed that the high activity of the Pt/P25 catalyst is due to the high electron density of the Pt particles. They behave as Lewis base sites for reductive deprotonation of aniline, thus promoting efficient aniline oxidation. The Pt/P25 catalyst, when photoirradiated at a low temperature (~283 K), produces nitrosobenzene with a very high selectivity (90%).

RESULTS AND DISCUSSION

Preparation and Properties of the Catalyst. The Pt/P25 catalyst was prepared by impregnation of Pt precursors followed by reduction with hydrogen (H_2).[31,32] P25 TiO_2 particles (particle size, 24 nm; BET surface area, 57 $m^2\ g^{-1}$; anatase/rutile ratio, 82/18) were added to water containing H_2PtCl_6, and the solvents were removed by evaporation during vigorous stirring. The resultant was calcined in air and reduced under a H_2 flow at 673 K, affording Pt_x/P25 as brown powders, where x denotes the amount of Pt loaded [x (weight percent) = $Pt/(Pt + TiO_2) \times 100$]. Figure 1a shows a typical transmission electron microscopy (TEM) image of the Pt_2/P25 catalyst. Pt nanoparticles are highly dispersed on the support. The average diameter of the Pt particles was determined to be 3.1 nm (Figure 1b). As shown in Figure 2, the diffuse-reflectance UV−vis spectrum of Pt_2/P25 exhibits a broad absorption band at $\lambda >$ 400 nm, assigned to the interband transition of Pt particles.[33]

Photocatalytic Activity. We performed photocatalytic oxidation of aniline by stirring a toluene solution (5 mL) containing aniline (1 mmol) and catalyst (20 mg) with O_2 (1 atm) under photoirradiation at $\lambda >$ 450 nm by a Xe lamp. The temperature of the solution was kept rigorously at 298 ± 0.5 K by a digitally controlled water bath. Figure 3 summarizes the amount of products formed by a 12 h photoreaction. It must be noted that gas chromatography (GC) analysis of the resulting solution for all of the systems detected only nitrosobenzene and azobenzene. With bare P25 TiO_2, almost no reaction occurs. In contrast, the Pt_2/P25 catalyst produces nitrosobenzene (9.7 μmol) with a minor amount of azobenzene (2.5 μmol). Although Pt nanoparticles exhibit catalytic activity for aerobic

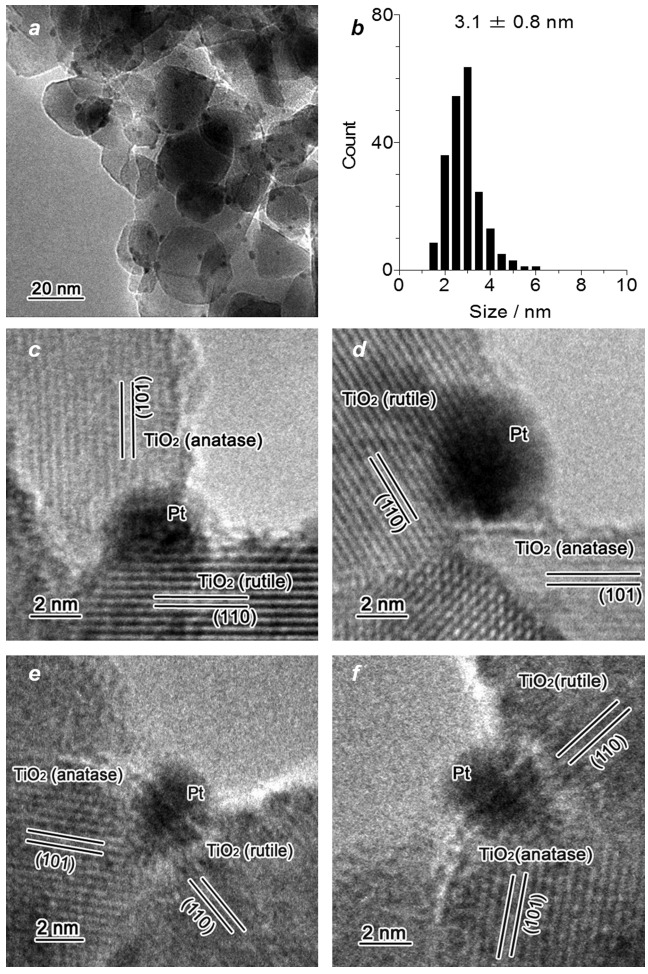

Figure 1. (a) Typical TEM image of the Pt_2/P25 catalyst and (b) size distribution of metal particles. (c−f) High-resolution TEM images of the catalyst. Anatase (101) and rutile (110) phases were identified by their lattice spacings (3.52 and 3.25 nm, respectively).

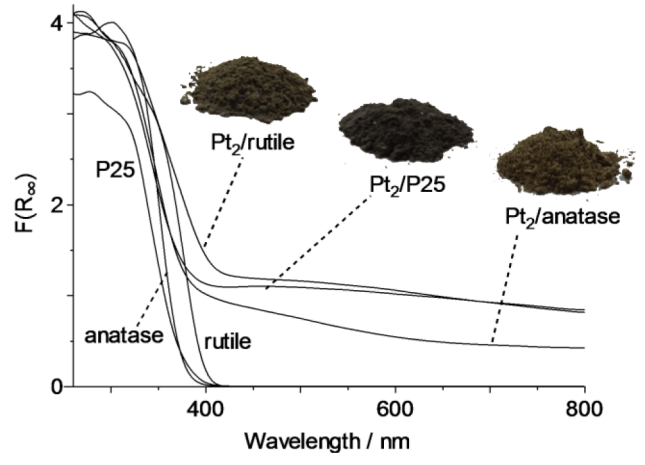

Figure 2. Diffuse-reflectance UV−vis spectra of the supports and catalysts.

oxidation even under the dark condition,[34,35] the Pt_2/P25 catalyst, when reacted under the dark condition, gave only a minor amount of products. An increase in temperature enhances the reaction even under the dark condition, but azobenzene is produced as a main product because of the

dx.doi.org/10.1021/cs500447n | ACS Catal. 2014, 4, 2418−2425

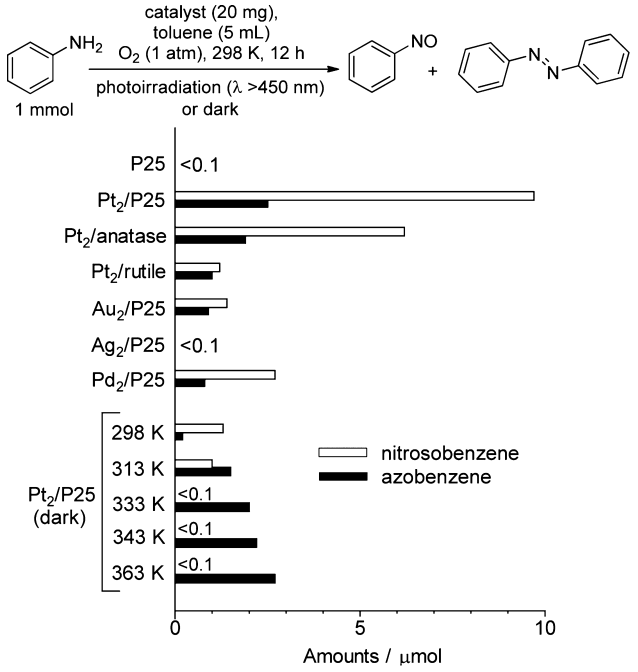

Figure 3. Amounts of (white) nitrosobenzene and (black) azobenzene produced by aerobic oxidation of aniline with respective catalysts in the dark or under visible light irradiation (λ > 450 nm; light intensity at 450−800 nm, 16.8 mW cm^{-2}). Diffuse-reflectance UV−vis spectra for Au, Pd, and Ag catalysts are summarized in Figure S1 of the Supporting Information.

condensation of aniline with the formed nitrosobenzene enhanced at higher temperatures.[13] These data suggest that visible light irradiation of the Pt/P25 catalyst at room temperature successfully promotes aerobic oxidation of aniline and selectively produces nitrosobenzene.

To clarify the effect of TiO_2 support, Pt particles were loaded on anatase TiO_2 (Japan Reference Catalyst JRC-TIO-1; average particle size, 21.1 nm; BET surface area, 81 m^2 g^{-1}) and rutile TiO_2 (Japan Reference Catalyst JRC-TIO-6; average particle size, 15 nm; BET surface area, 104 m^2 g^{-1}). As shown in Figure S2 of the Supporting Information, the sizes of Pt particles on these supports were determined to be 3.4 and 2.9 nm, respectively, both of which are similar to those of Pt_2/P25 [3.1 nm (Figure 1b)]. As shown in Figure 3, both Pt_2/anatase and Pt_2/rutile catalysts, however, show photocatalytic activity lower than that of Pt_2/P25. In addition, as shown in Figure S3 of the Supporting Information, Pt particles supported on other anatase and rutile TiO_2 particles with different particle sizes and surface areas also exhibit catalytic activity lower than that of Pt_2/P25. These data suggest that P25 TiO_2 is the support exhibiting the best photocatalytic performance. It is also noted that, as shown in Figure 3, Au, Ag, and Pd particles, when loaded on P25, exhibit activity much lower than that of Pt_2/P25, although these metal particles are also activated by visible light absorption via the intraband (Au[36,37] and Ag[38,39]) or interband (Pd[40,41]) transitions. These findings suggest that Pt particles loaded on P25 TiO_2 promote efficient aerobic oxidation of aniline under visible light irradiation. In addition, as shown in Figure 4, Pt_2/P25 maintains its activity even after prolonged photoirradiation (~48 h), suggesting that the catalyst scarcely loses its activity during the photoreaction.

Transfer of an Electron from Photoactivated Pt Particles to TiO_2. As shown in Scheme 1, in the Pt/P25

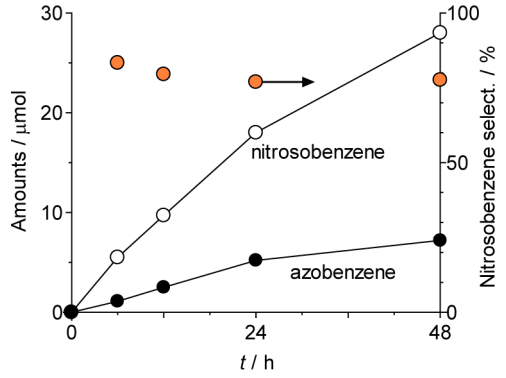

Figure 4. Time-dependent change in the amount of products and nitrosobenzene selectivity during photocatalytic reaction of aniline with Pt_2/P25. The reaction conditions are identical to those described in the legend of Figure 3.

system, photoactivated Pt particles transfer their e$^-$ to TiO_2, and the e$^-$ reduces O_2 on its surface. This is confirmed by electron spin resonance (ESR) analysis of the catalysts measured at 77 K after treatment of the sample with O_2 at 298 K under visible light irradiation (λ > 450 nm; 3 h) according to the procedure described previously (λ > 450 nm; 1 h).[24] As shown in Figure 5a (black), the Pt_2/P25 catalyst treated with O_2 in the dark shows almost no signal. Visible light

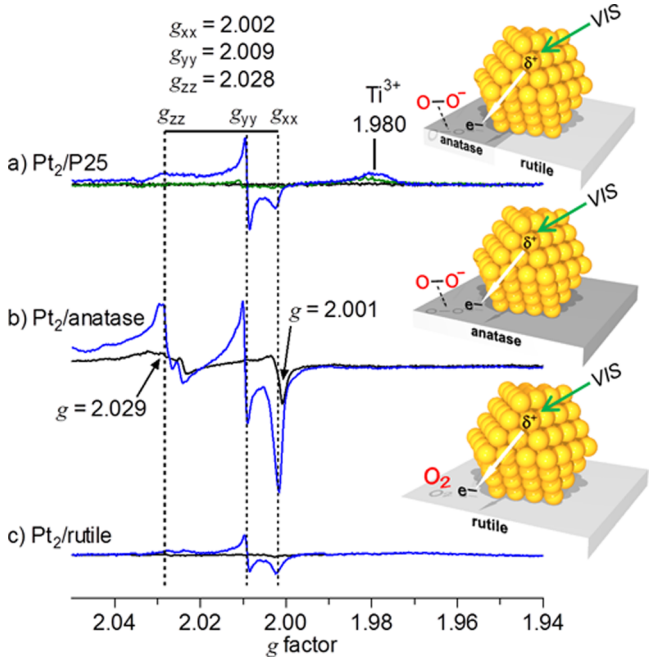

Figure 5. ESR spectra of respective catalysts measured at 77 K. The catalysts were treated at 298 K with 20 Torr of O_2 (black) in the dark or (blue) under visible light irradiation for 3 h. After evacuation, the samples were measured at 77 K. The green spectrum in panel a was obtained as follows. Aniline (7.5×10^{-2} Torr) was added at 298 K to the sample treated with O_2 under visible light irradiation and left for 10 min. After evacuation, the sample was measured at 77 K. The signals observed for the Pt/anatase sample (b) under the dark condition (g = 2.029 and 2.001) are assigned to O^- formed via a dissociative adsorption of O_2 onto the oxygen vacancy sites of the anatase TiO_2 surface, which was also observed for bare anatase TiO_2.[24] The broad g = 1.980 signal (spectrum a) is assigned to the Ti^{3+} species formed on rutile TiO_2.[45]

dx.doi.org/10.1021/cs500447n | ACS Catal. 2014, 4, 2418−2425

irradiation of this sample (blue), however, creates distinctive signals assigned to a superoxide-type oxygen anion (O_2^-; g_{xx} = 2.002, g_{yy} = 2.009, g_{zz} = 2.028) stabilized on the TiO_2 surface.[42] This suggests that photoactivated Pt particles indeed transfer e^- to TiO_2, and the e^- reduces O_2 on its surface. As shown in spectra b and c of Figure 5 (blue), photoirradiation of Pt_2/anatase creates much stronger O_2^- signals, whereas Pt_2/rutile shows very weak signals, as also observed in our previous work.[24] The weak O_2^- signals on the Pt/rutile catalyst exist because, as reported,[24,43] the transfer of an electron from photoactivated Pt particles to rutile TiO_2 is difficult and the rutile surface is inactive for O_2 reduction. The signal intensity of Pt/P25 is weaker than that of Pt/anatase because the Pt particles on P25 TiO_2 are located at the interface between anatase and rutile particles. This is confirmed by a high-resolution TEM image of the Pt/P25 catalyst. As shown in Figure 1c–f, Pt particles are indeed located at the anatase–rutile interface and show well-defined contact surfaces consisting of Pt/anatase/rutile phases. As a result of this, the smooth transfer of e^- from photoactivated Pt particles to anatase is suppressed, resulting in inefficient O_2 reduction.[44−47] The obtained ESR results suggest that the efficiency for photoinduced charge separation on Pt/P25 is lower than that on Pt/anatase. However, as shown in Figure 3, the photocatalytic activity of Pt/P25 is much higher.

High Electron Density of Pt Particles on Pt/P25. During the oxidation of aniline, deprotonation of aniline is the rate-determining step. The anilino anion formed via the deprotonation by the Lewis base is oxidized very efficiently.[48] As shown in Figure 3, photoreaction of aniline with Pt_2/anatase catalyst produces 6.2 μmol of nitrosobenzene with 1.9 μmol of azobenzene. Addition of triethylamine (1 mmol), which behaves as a base or a sacrificial reagent for photocatalytic reaction, to this system significantly enhances the reaction (producing 34 μmol of nitrosobenzene with 2.0 μmol of azobenzene). In contrast, addition of 2-PrOH (1 mmol), which does not behave as a base but acts as a sacrificial reagent, scarcely enhances the reaction (9.5 μmol of nitrosobenzene with 0.4 μmol of azobenzene). This clearly suggests that deprotonation of aniline by the base is indeed the rate-determining step for aniline photooxidation.

In the Pt/P25 system, Pt nanoparticles located at the interface between anatase and rutile phases possess high electron density and behave as the Lewis base site for reductive deprotonation of aniline. This thus promotes efficient photooxidation of aniline. The high electron density of Pt particles on P25 TiO_2 is confirmed by XPS analysis. As shown in Figure 6, the XPS chart of Pt/P25 shows Pt 4f 5/2 and 7/2 peaks at 73.5 and 70.1 eV, respectively. In contrast, both Pt/anatase and Pt/rutile catalysts exhibit these peaks at higher binding energies. This suggests that Pt particles on P25 TiO_2 indeed possess higher electron density.

The high electron density of Pt particles on P25 TiO_2 is due to the strong Pt–support interaction. As shown in Figure 1b and Figure S2 of the Supporting Information, Pt_2/P25, Pt_2/anatase, and Pt_2/rutile catalysts contain Pt particles with similar diameters (3.1, 3.4, and 2.9 nm, respectively), suggesting that the size of Pt particles does not affect the position of Pt XPS peaks. The Pt peaks of Pt/P25 at lower binding energies (Figure 6) therefore exist because a larger number of electrons on P25 TiO_2 are transferred to Pt at the interface. The position of Pt peaks usually depends on the Fermi level of the semiconductor; a semiconductor with a more negative Fermi

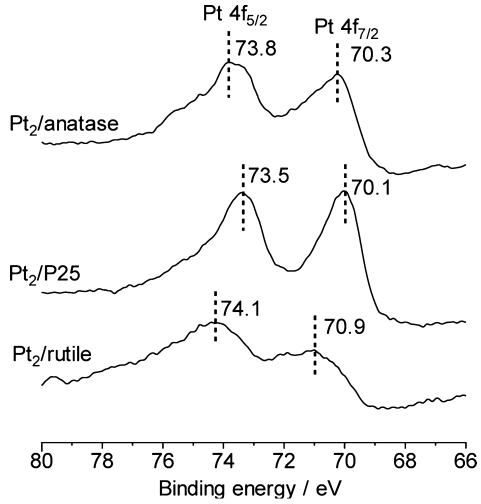

Figure 6. XPS chart (Pt 4f level) for catalysts. The data for other anatase and rutile catalysts are summarized in Figure S4 of the Supporting Information.

level transfers its electrons to Pt more efficiently and shows Pt XPS peaks at lower binding energies.[49,50] Rutile TiO_2 has a Fermi level more negative than that of anatase.[51] However, as shown in Figure 6 and Figure S4 of the Supporting Information, the Pt peaks for Pt/rutile catalysts appear at a binding energy higher than that of the Pt/anatase catalyst because the anatase surface is strongly associated with Pt particles, as supported by DFT calculations,[52] and transfers the electrons to Pt more efficiently.[53] In contrast, Pt/P25 shows Pt peaks at a binding energy lower than that of Pt/anatase (Figure 6). As reported,[22,54] metal nanoparticles such as Au are highly stabilized when they are located at the anatase–rutile interface. The strong Pt–support interaction of Pt/P25 therefore probably enhances the transfer of the electron from the support to Pt. This thus increases the electron density of Pt nanoparticles.

Lewis Base Activity of Pt Particles on the Pt/P25 Catalyst. The deprotonation of aniline promoted by Pt particles on the P25 support is confirmed by DRIFT analysis. Figure 7 shows the DRIFT spectra of aniline adsorbed onto the respective catalysts in the gas phase at 298 K. As shown in Figure 7a, the aniline adsorbed onto bare P25 shows two absorption bands at 3292 and 3245 cm^{-1}, which are assigned to the antisymmetric stretching vibration (ν_{anti}) and the symmetric stretching vibration (ν_{sym}) of the -NH_2 group, respectively.[55] As shown in spectra c and d of Figure 7, aniline when adsorbed onto the Pt/anatase and Pt/rutile catalysts also shows similar signals. However, in the case of Pt/P25 (Figure 7b), a new band appears at a higher wavenumber (3323 cm^{-1}). This indicates that some of the aniline molecules adsorbed onto the Pt particles on P25 are transformed to the species with a stronger (shorter) N–H bond.[56] Figure S5 of the Supporting Information shows the IR spectra of aniline measured in a CCl_4 solution. Distinctive ν_{anti} and ν_{sym} bands for -NH_2 groups appear at 3478 and 3395 cm^{-1}, respectively. In contrast, addition of 30 equiv of triethylamine to this solution creates a new band at a higher wavenumber (3511 cm^{-1}), which is assigned to the N–H vibrational band strengthened via deprotonation by the base.[57] The obtained band is similar to that obtained on the Pt/P25 catalyst (Figure 7b). These data clearly suggest that Pt particles on the P25 support indeed

dx.doi.org/10.1021/cs500447n | ACS Catal. 2014, 4, 2418–2425

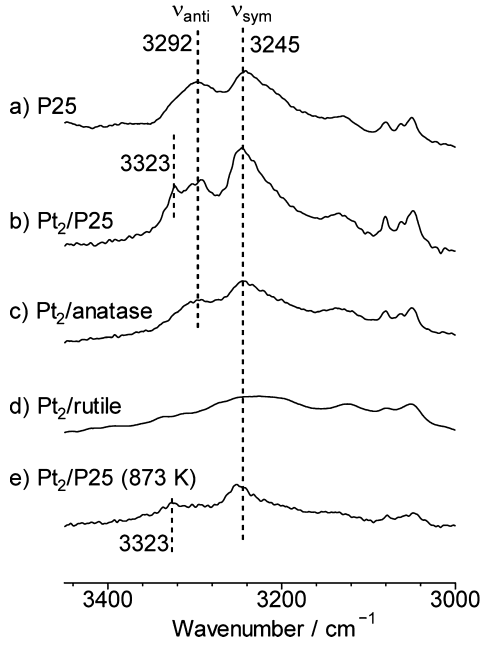

Figure 7. DRIFT spectra of aniline adsorbed, in the gas phase at 298 K on (a) bare P25, (b) Pt_2/P25, (c) Pt_2/anatase, (d) Pt_2/rutile, and (e) Pt_2/P25 prepared at 873 K. The catalyst was evacuated (6.8×10^{-3} Torr) at 423 K for 3 h. Aniline (7.5×10^{-2} Torr) was introduced into the cell at 298 K, and the sample was left for 10 min. Measurement was then started.

Scheme 2. Proposed Mechanism for Aerobic Oxidation of Aniline on the Pt/P25 Catalyst under Visible Light Irradiation

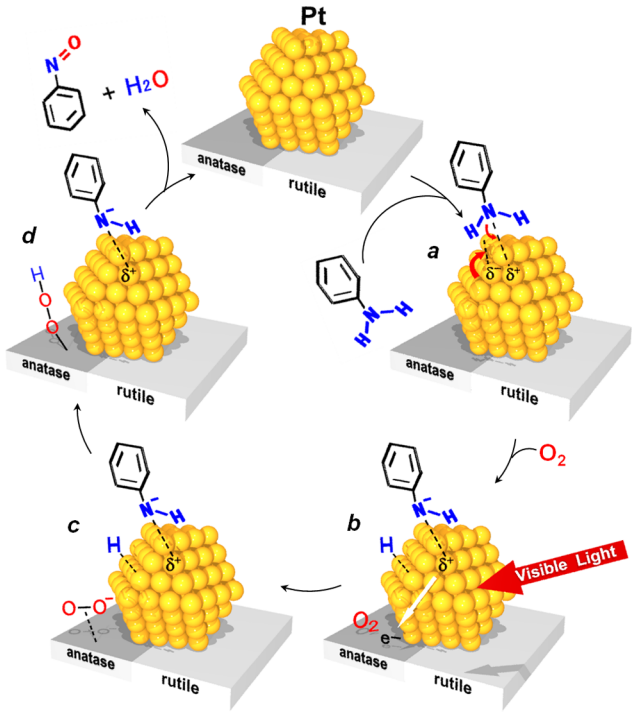

behave as Lewis base sites and promote reductive deprotonation of aniline.

On the basis of the findings described above, the mechanism for aerobic oxidation of aniline on the Pt/P25 catalyst is explained in Scheme 2. The reaction is initiated by deprotonation of aniline on the Lewis base site on Pt nanoparticles (a), producing anilino anion. Visible light absorption of Pt particles transfers their e^- to anatase (b). The e^- reduces O_2 and produces a superoxide anion (O_2^-) on the anatase surface (c). The O_2^- attracts the removed H atom of aniline and produces a hydroperoxide species (d), as is observed in related systems for oxidation of alcohols.[58,59] As shown in Figure 5a (blue), the ESR spectrum of Pt/P25 obtained by visible light irradiation with O_2 shows distinctive signals assigned to O_2^-. However, as shown by the green spectrum, addition of aniline to this sample completely quenches the O_2^- signal. This suggests that, as shown in Scheme 2 (c → d), the H atom removed by deprotonation of aniline on the Pt particles reacts with O_2^- and produces a hydroperoxide species. Subsequent reaction between the anilino anion and hydroperoxide species[58,59] gives rise to nitrosobenzene and water and completes the photocatalytic cycle.

Effects of the Amount of Pt and Particle Size. The catalytic activity for aerobic oxidation of aniline on Pt/P25 depends on the amount of Pt loaded. We prepared Pt_x/P25 catalysts with different Pt loadings [x (weight percent) = Pt/(Pt + P25) × 100 = 0.5, 1, 3, and 4]. As shown in Figure S6 of the Supporting Information, the sizes of Pt particles on the $Pt_{0.5}$/P25 and Pt_4/P25 catalysts were determined by TEM observations to be 3.0 and 3.2 nm, respectively, which are similar to those on Pt_2/P25 (3.1 nm). This indicates that the amount of Pt loaded scarcely affects the Pt particle sizes. Figure 8a (bars) summarizes the amounts of nitrosobenzene and azobenzene produced by a 12 h photoreaction with respective catalysts. As shown by the orange symbols, the nitrosobenzene selectivities for the catalysts are similar (~80%). The amount of nitrosobenzene formed, however, depends on the amount of Pt loaded; the activity increases with Pt loadings (0.5−2 wt %) because the increase in the number of surface Pt atoms promotes efficient transfer of e^- to anatase and deprotonation of aniline. The activity, however, decreases with >2 wt % Pt loadings. As reported previously,[60] the increase in the amount of Pt loaded onto the semiconductor surface leads to an increase in the Schottky barrier height (ϕ_B), because of the decrease in the Fermi level of the semiconductor. The increased ϕ_B probably suppresses the transfer of e^- from photoactivated Pt particles to anatase, resulting in decreased photocatalytic activity.

The Pt particle size also affects catalytic activity. The Pt_2/P25 catalysts were prepared at different calcination and reduction temperatures (673, 773, and 873 K) while maintaining a 2 wt % Pt loading. As shown in Figure S6 of the Supporting Information, the size of Pt particles on the Pt/P25 catalyst prepared at 873 K is determined to be 6.7 nm, which is much larger than that prepared at 673 K (3.1 nm). This is due to the sintering of Pt particles by a high-temperature treatment.[24,25] Figure 8b shows the results obtained via a 12 h photoreaction with respective catalysts. Although the nitrosobenzene selectivities are similar, the activity significantly decreases with an increase in the size of Pt particles because the number of surface Pt atoms decreases with an increase in the size of Pt particles.[61] This suppresses the transfer of e^- from photoactivated Pt atoms to anatase[24] as well as deprotonation of aniline, resulting in decreased photocatalytic activity. Figure 7e shows the DRIFT spectrum of aniline adsorbed onto the Pt_2/P25 catalyst prepared at 873 K. The signal intensity at 3323 cm^{-1}, assigned to the anilino anion, is much weaker than the

dx.doi.org/10.1021/cs500447n | ACS Catal. 2014, 4, 2418−2425

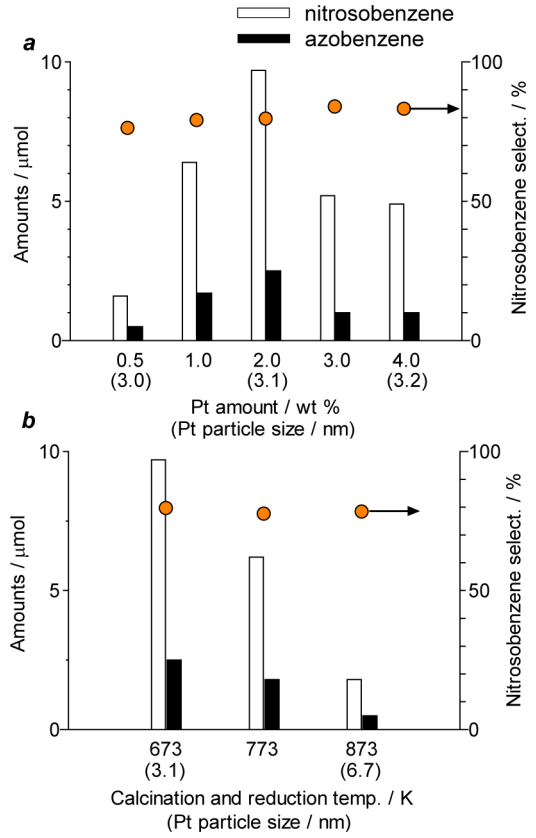

Figure 8. Effect of (a) the amount of Pt loaded and (b) calcination and reduction temperature on the amounts of (white) nitrosobenzene and (black) azobenzene produced during photocatalytic oxidation of aniline with Pt/P25. Orange symbols denote the nitrosobenzene selectivity. The calcination and reduction temperature employed for the preparation of catalysts (a) is 673 K, and the Pt loading of the catalysts (b) is 2 wt %. Reaction conditions are identical to those described in the legend of Figure 3.

catalyst prepared at 673 K (Figure 7b). This suggests that the catalyst with larger Pt particles is less active for deprotonation of aniline. The findings described above clearly indicate that the Pt/P25 catalyst containing 2 wt % Pt particles with ∼3 nm diameters exhibits the best catalytic performance for aerobic oxidation of aniline.

Effect of Reaction Temperature on Selectivity. Photocatalytic oxidation of aniline on the Pt/P25 catalyst produces azobenzene as a byproduct, which is formed by subsequent condensation of aniline and the formed nitrosobenzene.[13] The formation of azobenzene strongly depends on the reaction temperature. Figure 9 summarizes the amounts of nitrosobenzene and azobenzene produced by a 12 h photoreaction at different temperatures. An increase in reaction temperature significantly decreases the amount of nitrosobenzene formed, along with an increase in the level of azobenzene formation, because of the enhanced condensation of aniline and the formed nitrosobenzene. The nitrosobenzene selectivity at 343 K is only 13%. In contrast, at lower temperatures (<298 K), nitrosobenzene is selectively produced; the selectivity at 283 K is increased to 90%. These data suggest that photoreaction at low temperatures suppresses the condensation of aniline with the product nitrosobenzene, thus facilitating selective nitrosobenzene formation.

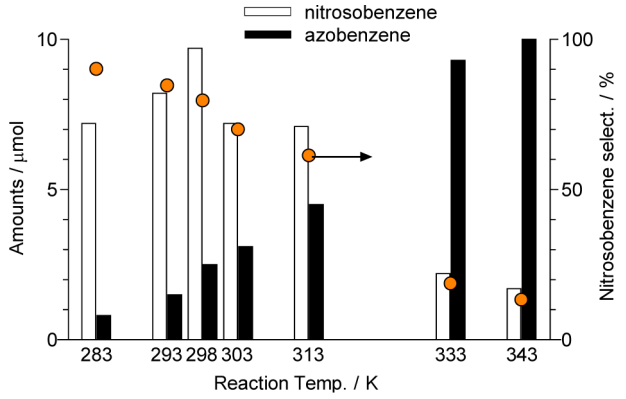

Figure 9. Effect of reaction temperature on the amounts of (white) nitrosobenzene and (black) azobenzene produced during photocatalytic oxidation of aniline. Orange symbols denote the nitrosobenzene selectivity. Reaction conditions are identical to those described in the legend of Figure 3.

CONCLUSION

We found that the Pt/P25 catalyst promotes efficient aerobic oxidation of aniline to nitrosobenzene under visible light irradiation (>450 nm). Pt nanoparticles activated by visible light transfer their e^- to the TiO_2 conduction band. The positive charge that remained on the Pt surface oxidizes aniline, and the e^- on TiO_2 reduces O_2, promoting aerobic oxidation of aniline. The high activity of Pt/P25 is ascribed to the high Lewis basicity of Pt particles due to the strong Pt−support interaction at the anatase−rutile interfaces. These Pt particles promote reductive deprotonation of aniline, resulting in the efficient photooxidation of aniline. The catalytic activity of Pt/P25 strongly depends on the amount and size of Pt particles. The catalyst containing 2 wt % Pt particles with ∼3 nm diameters exhibits the best catalytic performance. The selectivity for nitrosobenzene formation also depends on the reaction temperature; reaction at low temperatures suppresses condensation of aniline with the formed nitrosobenzene and produces nitrosobenzene with a very high selectivity (∼90%).

EXPERIMENTAL SECTION

Materials. All reagents used were purchased from Wako, Tokyo Kasei, and Sigma-Aldrich and used without further purification. Water was purified by the Milli-Q system. Anatase TiO_2 (JRC-TIO-1), P25 (JRC-TIO-4), and rutile TiO_2 (JRC-TIO-6; particle size, 15 nm; BET surface area, 104 $m^2\ g^{-1}$) were kindly supplied by the Catalyst Society of Japan.

Pt_x/TiO_2. The catalysts with different Pt loadings [x (weight percent) = 0.5, 1, 2, 3, or 4] were prepared as follows. TiO_2 (1 g) was added to water (40 mL) containing $H_2PtCl_6{\cdot}6H_2O$ (13.3, 26.8, 54.2, 82.1, or 110.6 mg). The solvents were removed by evaporation at 353 K with vigorous stirring for 12 h. The obtained powders were calcined under air flow and then reduced under H_2 flow at the identical temperature. Unless otherwise noted, these treatments were conducted at 673 K. The heating rate was 2 K min^{-1}, and the holding time at the designated temperature was 2 h.

$M_2/P25$. The catalysts with 2 wt % metal particles (M = Ag or Pd) were prepared as follows. P25 TiO_2 (1 g) was added to water (40 mL) containing $AgNO_3$ (32.1 mg) or $Pd(NO_3)_2$ (44.2 mg). The solvents were removed by evaporation with vigorous stirring at 353 K for 12 h. The resulting powders were calcined at 673 K for 2 h under air flow and reduced at 673 K

dx.doi.org/10.1021/cs500447n | ACS Catal. 2014, 4, 2418−2425

for 2 h under H_2 flow. The Au_2/P25 catalyst was prepared by the deposition–precipitation method.[22] P25 TiO_2 (1 g) was added to water (50 mL) containing $HAuCl_4 \cdot 4H_2O$ (45.8 mg). The pH of the solution was adjusted to ∼7 with 1 mM NaOH, and the solution was stirred at 353 K for 3 h. The particles were recovered by centrifugation, washed with water, and dried at 353 K for 12 h. The powder was calcined under air flow, where the heating rate was 2 K min^{-1} and the holding time at 673 K was 2 h.

Photoreaction. The catalyst (20 mg) was added to toluene (5 mL) containing aniline within a Pyrex glass tube (φ, 12 mm; capacity, 20 mL). The tube was sealed with a rubber septum cap. The catalyst was dispersed by ultrasonication for 5 min, and O_2 was bubbled through the solution for 5 min. The tube was immersed in a temperature-controlled water bath (298 ± 0.5 K). The tube was photoirradiated with magnetic stirring using a 2 kW Xe lamp (Ushio Inc.).[62] The light was filtered through a glass filter (CS3-72, Kopp Glass Inc.) to give >450 nm light, where the light intensity at 450–800 nm was 16.8 mW cm^{-2}. After the reaction, the catalyst was recovered by centrifugation. The liquid phase products were analyzed by GC and free induction decay (Shimadzu, GC-1700).

ESR Measurement. The spectra were recorded at the X-band using a Bruker EMX-10/12 spectrometer with a 100 kHz magnetic field modulation at a microwave power level of 10.0 mW, where microwave power saturation of the signal does not occur.[63] The magnetic field was calibrated with 1,1′-diphenyl-2-picryl-hydrazyl (DPPH). The catalyst (20 mg) was placed in a quartz ESR tube and the tube evacuated at 423 K for 3 h. After the tube had been cooled to room temperature, O_2 (20 Torr) was introduced into the tube and the tube kept for 3 h at 298 K. The tube was photoirradiated for 3 h at 298 K. The tube was then evacuated for 10 min to remove the excess of O_2 and subjected to analysis at 77 K.

DRIFT Analysis. The spectra were measured on a FTIR 610 system equipped with a DR-600B *in situ* cell (Jasco Corp.).[64] The catalyst (50 mg) was placed in a DR cell and the cell evacuated (6.8×10^{-3} Torr) at 423 K for 3 h. Aniline (7.5×10^{-2} Torr) was introduced into the cell at 298 K, and measurement was started.

Other Analysis. TEM observations were made using a JEOL Tecnai G2 20ST analytical electron microscope operated at 200 kV.[65] XPS analysis was performed using a JEOL JPS9000MX spectrometer with Mg Kα radiation as the energy source. Diffuse-reflectance UV–vis spectra were measured on an UV–vis spectrometer (Jasco Corp.; V-550 with Integrated Sphere Apparatus ISV-469) with $BaSO_4$ as a reference. IR spectra were recorded at room temperature using an FTIR-610 spectrometer (Jasco Corp.) with a liquid sample cell with a CaF_2 window.[66]

■ ASSOCIATED CONTENT

Supporting Information

Diffuse-reflectance UV–vis spectra of catalysts (Figure S1), TEM images of anatase and rutile catalysts and size distribution of Pt particles (Figure S2), reaction results (Figure S3), XPS chart for catalysts (Figure S4), IR spectra for aniline (Figure S5), TEM images of Pt/P25 catalysts and size distribution of Pt particles (Figure S6), and XRD patterns of catalysts (Figure S7). This material is available free of charge via the Internet at http://pubs.acs.org.

■ AUTHOR INFORMATION

Corresponding Author

*E-mail: shiraish@cheng.es.osaka-u.ac.jp.

Notes

The authors declare no competing financial interest.

■ ACKNOWLEDGMENTS

This work was supported by a Grant-in Aid for Scientific Research (23360349) from the Ministry of Education, Culture, Sports, Science and Technology, Japan (MEXT).

■ REFERENCES

(1) Yamamoto, H.; Momiyama, N. *Chem. Commun.* **2005**, 3514–3525.
(2) Adam, W.; Krebs, O. *Chem. Rev.* **2003**, *103*, 4131–4146.
(3) Zhao, D.; Johansson, M.; Backvall, J.-E. *Eur. J. Org. Chem.* **2007**, 4431–4436.
(4) Defoin, A. *Synthesis* **2004**, *5*, 706–710.
(5) Gowenlock, B. G.; Richer-Addo, G. B. *Chem. Rev.* **2004**, *104*, 3315–3340.
(6) Meenakshisundaram, S.; Selvaraju, M.; Gowda, N. M. M.; Rangappa, K. S. *J. Chem. Kinet.* **2005**, *37*, 649–657.
(7) Priewish, B.; Braun, K. R. *J. Org. Chem.* **2005**, *70*, 2350–2352.
(8) Møller, E. R.; Jørgensen, K. A. *J. Am. Chem. Soc.* **1993**, *115*, 11814–11822.
(9) Sakaue, S.; Tsubakino, T.; Nishiyama, Y.; Ishii, Y. *J. Org. Chem.* **1993**, *58*, 3633–3638.
(10) Grirrane, A.; Corma, A.; Garcia, H. *Science* **2008**, *322*, 1661–1664.
(11) Kus, N. S. *Monatsh. Chem.* **2010**, *141*, 1089–1091.
(12) Perez, Y.; Aprile, C.; Corma, A. *Catal. Lett.* **2010**, *134*, 204–209.
(13) Biradar, A. V.; Kotbagi, T. V.; Dongare, M. K.; Umbarkar, S. B. *Tetrahedron Lett.* **2008**, *49*, 3616–3619.
(14) Porta, F.; Pizzotti, M.; Cenini, S. *J. Org. Chem.* **1981**, *222*, 279–284.
(15) Fox, M. A. *Acc. Chem. Res.* **1983**, *16*, 314–321.
(16) Fox, M. A.; Dulay, M. T. *Chem. Rev.* **1993**, *93*, 341–357.
(17) Palmisano, G.; Augugliaro, V.; Pagliaro, M.; Palmisano, L. *Chem. Commun.* **2007**, 3425–3437.
(18) Shiraishi, Y.; Hirai, T. *J. Photochem. Photobiol., C* **2008**, *9*, 157–170.
(19) Karunakaran, C.; Senthilvelan, S.; Karuthapandian, S. *J. Photochem. Photobiol., A* **2005**, *172*, 207–213.
(20) Karunakaran, C.; Senthilvelan, S.; Karuthapandian, S. *Sol. Energy Mater. Sol. Cells* **2005**, *89*, 391–402.
(21) Karunakaran, C.; Senthilvelan, S. *J. Mol. Catal. A: Chem.* **2005**, *233*, 1–8.
(22) Tsukamoto, D.; Shiraishi, Y.; Sugano, Y.; Ichikawa, S.; Tanaka, S.; Hirai, T. *J. Am. Chem. Soc.* **2012**, *134*, 6309–6315.
(23) Sugano, Y.; Shiraishi, Y.; Tsukamoto, D.; Ichikawa, S.; Tanaka, S.; Hirai, T. *Angew. Chem., Int. Ed.* **2013**, *52*, 5295–5299.
(24) Shiraishi, Y.; Tsukamoto, D.; Sugano, Y.; Shiro, A.; Ichikawa, S.; Tanaka, S.; Hirai, T. *ACS Catal.* **2012**, *2*, 1984–1992.
(25) Shiraishi, Y.; Sakamoto, H.; Sugano, Y.; Ichikawa, S.; Hirai, T. *ACS Nano* **2013**, *7*, 9287–9297.
(26) Schottky, W. *Z. Phys.* **1939**, *113*, 367–414.
(27) Hao, Q.; Juluri, B. K.; Zheng, Y. B.; Wang, B.; Chiang, I.-K.; Jensen, L.; Crespi, V.; Eklund, P. C.; Huang, T. J. *J. Phys. Chem. C* **2010**, *114*, 18059–18066.
(28) Sachtleben Chemie GmbH, June 24, 1994.
(29) Otani, B.; Prieto-Mahaney, O. O.; Li, D.; Abe, P. *J. Photochem. Photobiol., A* **2010**, *226*, 179–182.
(30) Shiraishi, Y.; Hirakawa, H.; Togawa, Y.; Sugano, Y.; Ichikawa, S.; Hirai, T. *ACS Catal.* **2013**, *3*, 2318–2326.
(31) Shiraishi, Y.; Ikeda, M.; Tsukamoto, D.; Tanaka, S.; Hirai, T. *Chem. Commun.* **2011**, *47*, 4811–4813.

(32) Shiraishi, Y.; Takeda, Y.; Sugano, Y.; Ichikawa, S.; Tanaka, S.; Hirai, T. *Chem. Commun.* **2011**, *47*, 7863−7865.
(33) Bigall, N. C.; Hartling, T.; Klose, M.; Simon, P.; Eng, L. M.; Eychmuller, A. *Nano Lett.* **2008**, *8*, 4588−4592.
(34) Proch, S.; Herrmannsdörfer, J.; Kempe, R.; Kern, C.; Jess, A.; Seyfarth, L.; Senker, J. *Chem.—Eur. J.* **2008**, *14*, 8204−8212.
(35) Hong, H.; Hu, L.; Li, M.; Zheng, J.; Sun, X.; Lu, X.; Cao, X.; Lu, J.; Gu, H. *Chem.—Eur. J.* **2011**, *17*, 8726−8730.
(36) He, Y.; Zeng, T. *J. Phys. Chem. C* **2010**, *114*, 18023−18030.
(37) Fatti, N. D.; Voisin, C.; Achermann, M.; Tzortzakis, S.; Christofilos, D.; Vallee, F. *Phys. Rev. B* **2000**, *61*, 16956−16966.
(38) Mendoza, B. S. *Phys. Rev. B* **1999**, *60*, 14334−14340.
(39) Link, S.; Burda, C.; Wang, Z. L.; El-Sayed, M. A. *J. Chem. Phys.* **1999**, *111*, 1255−1264.
(40) Kirillova, M. M.; Makhnev, A. A.; Shreder, E. I.; Dyakina, V. P.; Gorina, N. B. *Phys. Status Solidi* **1995**, *187*, 231−240.
(41) Morkel, M.; Unterhalt, H.; Kluner, T.; Rupprechter, G.; Freund, H. J. *Surf. Sci.* **2005**, *586*, 146−156.
(42) Anpo, M.; Che, M.; Fubini, B.; Garrone, E.; Giamello, E.; Paganini, M. C. *Top. Catal.* **1999**, *8*, 189−198.
(43) Ohno, T.; Sarukawa, K.; Matsumura, M. *J. Phys. Chem. B* **2001**, *105*, 2417−2420.
(44) As shown in Figure 5a (black), the Pt/P25 catalyst when left in the dark with O_2 shows almost no signal at g values of <1.99. Visible light irradiation of the catalyst (blue), however, creates signals assigned to Ti^{3+} species formed on rutile TiO_2.[45] This suggests that visible light absorption by Pt particles transfers their e^- to the TiO_2 support. In contrast, visible light irradiation of the Pt/anatase catalyst (Figure 5b) shows almost no Ti^{3+} signal. This is probably because the e^- transferred from photoactivated Pt particles to anatase are efficiently consumed by the reduction of O_2. This agrees well with the strong O_2^- signals. Visible light irradiation of the Pt/rutile catalyst (Figure 5c) also shows almost no Ti^{3+} signal, but the intensity of the O_2^- signal is much weaker. This suggests that, in the Pt/rutile system, the transfer of e^- from photoactivated Pt to rutile is difficult. In contrast, visible light irradiation of the Pt/P25 catalyst (Figure 5a) creates Ti^{3+} species formed on the rutile TiO_2, although the transfer of e^- from photoactivated Pt to rutile is difficult. This can be rationalized by the transfer of e^- from anatase to rutile, as is often observed for related P25 systems (for example, refs 47 and 48). As reported previously,[43] the e^- on the rutile surface are inactive for O_2 reduction; therefore, the Ti^{3+} species on rutile TiO_2 remain even in the presence of O_2.
(45) Okumura, M.; Coronado, J. M.; Soria, J.; Haruta, M.; Conesa, J. C. *J. Catal.* **2001**, *203*, 168−174.
(46) Ohno, T.; Tokieda, K.; Higashida, S.; Matsumura, M. *Appl. Catal., A* **2003**, *244*, 383−391.
(47) Komaguchi, K.; Nakano, H.; Araki, A.; Harima, Y. *Chem. Phys. Lett.* **2006**, *428*, 338−342.
(48) Zhou, C.; Han, J.; Song, G.; Guo, R. *Eur. Polym. J.* **2008**, *44*, 2850−2858.
(49) Horsley, J. A. *J. Am. Chem. Soc.* **1979**, *101*, 2870−2874.
(50) Sexton, B. A.; Hughes, A. E.; Foger, K. *J. Catal.* **1982**, *77*, 85−93.
(51) Zhang, X.; Lin, Y.; He, D.; Zhang, J.; Fan, Z.; Xie, T. *Chem. Phys. Lett.* **2011**, *504*, 71−75.
(52) Gong, X.-Q.; Selloni, A.; Dulub, O.; Jacobson, P.; Diebold, U. *J. Am. Chem. Soc.* **2008**, *130*, 370−381.
(53) Bu, Y.; Chen, Z.; Li, W. *Appl. Catal., B* **2014**, *144*, 622−630.
(54) Akita, T.; Lu, P.; Ichikawa, S.; Tanaka, K.; Haruta, M. *Surf. Interface Anal.* **2001**, *31*, 73−78.
(55) Evans, J. C. *Spectrochim. Acta* **1960**, *16*, 428−442.
(56) Brown, E. V.; Kipp, W. H. *J. Org. Chem.* **1971**, *36*, 170−173.
(57) Maeda, Y.; Higuchi, T.; Ikeda, I. *Langmuir* **2000**, *16*, 7503−7509.
(58) Fukuto, J. M.; Di Stefano, E. W.; Burstyn, J. N.; Valentine, J. S.; Cho, A. K. *Biochemistry* **1985**, *24*, 4161−4167.
(59) Ishida, T.; Nagaoka, M.; Akita, T.; Haruta, M. *Chem.—Eur. J.* **2008**, *14*, 8456−8460.
(60) Uchihara, T.; Matsumura, M.; Yamamoto, A.; Tsubomura, H. *J. Phys. Chem.* **1989**, *93*, 5870−5874.
(61) The anatase-to-rutile phase transition of P25 TiO_2 upon calcination at higher temperatures is not the major factor for decreased photocatalytic activity. As shown in Figure S7 of the Supporting Information, XRD patterns indicated the anatase/rutile ratios of both Pt_2/P25 catalysts prepared by calcination at 673 and 773 K to be 81/19, which is similar to that of pure P25 TiO_2 (82/18), although calcination at 873 K increases the ratio to 75/25 by the thermal phase transition. As shown in Figure 8b, the catalyst prepared at 773 K showed activity lower than the activity of that prepared at 673 K, even though their anatase/rutile ratios are similar. This indicates that the phase transition of the P25 support is not the major factor in the decreased activity of the catalysts prepared at higher calcination temperatures.
(62) Shiraishi, Y.; Sugano, Y.; Tanaka, S.; Hirai, T. *Angew. Chem., Int. Ed.* **2010**, *49*, 1656−1660.
(63) Shiraishi, Y.; Saito, N.; Hirai, T. *J. Am. Chem. Soc.* **2005**, *127*, 12820−12822.
(64) Shiraishi, Y.; Togawa, Y.; Tsukamoto, D.; Tanaka, S.; Hirai, T. *ACS Catal.* **2012**, *2*, 2475−2481.
(65) Shiraishi, Y.; Tanaka, K.; Shirakawa, E.; Sugano, Y.; Ichikawa, S.; Tanaka, S.; Hirai, T. *Angew. Chem., Int. Ed.* **2013**, *52*, 8304−8308.
(66) Shiraishi, Y.; Matsunaga, Y.; Hirai, T. *Chem. Commun.* **2012**, *48*, 5485−5487.